BioOne COMPLETE

Mapping Plant Functional Groups in Subalpine Grassland of the Greater Caucasus

Authors: Anja Magiera, Hannes Feilhauer, Rainer Waldhardt, Martin Wiesmair, and Annette Otte

---

BioOne sees sustainable scholarly publishing as an inherently collaborative enterprise connecting authors, nonprofit publishers, academic institutions, research libraries, and research funders in the common goal of maximizing access to critical research.

Mapping Plant Functional Groups in Subalpine Grassland of the Greater Caucasus

Anja Magiera[1,2]*, Hannes Feilhauer[3], Rainer Waldhardt[1,2], Martin Wiesmair[1,2], and Annette Otte[1,2]

* Corresponding author: anja.magiera@agrar.uni-giessen.de

[1] Division of Landscape Ecology and Landscape Planning, Institute of Landscape Ecology and Resources Management, Justus-Liebig University Giessen, Heinrich-Buff-Ring 26-32, 35392 Giessen, Germany
[2] Center for International Development and Environmental Research (ZEU), Senckenbergstrasse 3, 35390 Giessen, Germany
[3] Institute of Geography, Friedrich-Alexander University Erlangen-Nürnberg, Wetterkreuz 15, 91058 Erlangen, Germany

Plant functional groups— in our case grass, herbs, and legumes—and their spatial distribution can provide information on key ecosystem functions such as species richness, nitrogen fixation, and erosion control.

Knowledge about the spatial distribution of plant functional groups provides valuable information for grassland management. This study described and mapped the distribution of grass, herb, and legume coverage of the subalpine grassland in the high-mountain Kazbegi region, Greater Caucasus, Georgia. To test the applicability of new sensors, we compared the predictive power of simulated hyperspectral canopy reflectance, simulated multispectral reflectance, simulated vegetation indices, and topographic variables for modeling plant functional groups. The tested grassland showed characteristic differences in species richness; in grass, herb, and legume coverage; and in connected structural properties such as yield. Grass (Hordeum brevisubulatum) was dominant in biomass-rich hay meadows. Herb-rich grassland featured the highest species richness and evenness, whereas legume-rich grassland was accompanied by a high coverage of open soil and showed dominance of a single species, Astragalus captiosus. The best model fits were achieved with a combination of reflectance, vegetation indices, and topographic variables as predictors. Random forest models for grass, herb, and legume coverage explained 36%, 25%, and 37% of the respective variance, and their root mean square errors varied between 12–15%. Hyperspectral and multispectral reflectance as predictors resulted in similar models. Because multispectral data are more easily available and often have a higher spatial resolution, we suggest using multispectral parameters enhanced by vegetation indices and topographic parameters for modeling grass, herb, and legume coverage. However, overall model fits were merely moderate, and further testing, including stronger gradients and the addition of shortwave infrared wavelengths, is needed.

Keywords: Remote sensing; subalpine grassland composition; random forest; spatial distribution of grass; grass cover; herb cover; legume cover; Georgia.

Introduction

Worldwide, high-mountain grasslands are species-rich habitats that include numerous endemic species (Körner 2004) but are commonly highly affected by natural and land use-triggered erosion, land degradation, and land use changes (eg Tasser and Tappeiner 2002; Lehnert et al 2014; Wiesmair et al 2016). The high species richness of subalpine to alpine grasslands results from, and is affected by, long-term agricultural use. During the last decades, central European mountain grassland communities have been altered by the introduction of modern farming practices in grassland management on the one hand, and by the abandonment of agricultural use on the other (Tasser and Tappeiner 2002). Traditional high-mountain land use systems with low input of system-specific organic fertilizers had greatly contributed to a distinct floristic pattern. This changed when mineral fertilizers and more effective agricultural techniques were introduced, making more intensive management regimes applicable to large grassland sites while modifying the traditional mowing and grazing regimes, as well as homogenizing floristic patterns (Homburger and Hofer 2012). The introduction of mineral nitrogen and phosphorus fertilizers caused the greatest change in the floristic composition of grassland and resulted in an increased abundance of ubiquitous species (Bühler and Roth 2011).

In contrast, the subalpine grassland in our study area, the Kazbegi region, Greater Caucasus, Georgia, has been traditionally managed without any mineral fertilizer application (Tephnadze et al 2014). Therefore, near-natural, species-rich, and quite distinct grassland types with

a strong relation to topography and land use type dominate the subalpine and alpine landscape of the Kazbegi region (Pyšek and Šrutek 1989; Nakhutsrishvili 1999; Tephnadze et al 2014). Species-rich grassland, characterized by a dense and vertically structured vegetation layer and a diverse and deep root system, contributes to the functioning of the high-mountain ecosystem, especially to erosion control (Pohl et al 2009; Körner 2003).

The legume content of grassland stands is closely linked to various ecosystem functions. By their ability to fix nitrogen, legumes influence the nitrogen pool within the soil system, which further affects the root system as well as biomass production and vegetation cover (Spehn et al 2002)—important factors for erosion mitigation (Tasser and Tappeiner 2002; Lehnert et al 2014; Wiesmair et al 2017). Therefore, detailed spatial knowledge about the distribution of plant functional groups (PFGs)—groups of plants (grasses, herbs, legumes) that share similar traits and perform similar ecosystem functions—provides valuable information for grassland management (Blondel 2003).

Previous studies indicate the feasibility of using remotely sensed imagery and topographic information to model grass, herb, and legume coverage (Zha et al 2003; Biewer, Erasmi, et al 2009; Biewer, Fricke, et al 2009; Himstedt et al 2009; Psomas et al 2011). However, studies using grass, herb, and legume coverage as a target variable have so far been limited to controlled systems, achieving best results with a homogenous yield. In contrast, our study was based on seminatural mountain grassland with varying yields and cover.

We characterized grassland composition and structure of the researched grassland types and subsequently modeled and mapped the PFGs' spatial distribution. We further tested whether hyperspectral reflectance (HR)—in our case from field spectrometric data—enhanced the model's quality. We therefore aimed to (1) model and map grass, herb, and legume coverage and (2) test whether simulated HR improved the model quality.

Study area

Steep slopes and a harsh continental climate characterize the high-mountain range of the Central Greater Caucasus, Georgia, and especially the environmental conditions of the isolated Kazbegi region (Figure 1). The Tergi River runs north; the main village, Stepantsminda (1700 masl), stretches along its banks. West of the river, Mount Kazbeg (5033 masl) rises as the highest summit in the region (Ketskhoveli et al 1975). The climate of the valley is relatively continental, with long, cool summers and winters with low snow cover. The mean annual temperature is 4.7°C, leading to a vegetation period of 5 to 6 months. The mean annual precipitation at 1850 masl amounts to 806 mm (Nakhutsrishvili 1999; Lichtenegger et al 2006). The bedrock of the study area comprises Jurassic

sediments (clay schists), quaternary volcanic rocks (andesite and dacite), and quaternary pyroclastic deposits and fluvial sediments. Younger, Pleistocene glacial sediments as well as Holocene peats can also be found (Akhalkatsi et al 2006). The main soil types on the higher part of slopes are shallow Leptosols, used mainly as pastures, whereas on the lower slopes and accumulation areas, depending on the bedrock, moderately deep Cambisols can be found; these are located mainly close to the villages, where they are used as meadows or potato fields (Tephnadze et al 2014).

The landscape is characterized by large, low-productivity, pastured grassland alternating with small remnants of birch forests (*Betula litwinowii*) and shrubberies. The grassland of north-facing slopes exhibits a relatively high biomass but is often characterized by unpalatable plant species such as *Veratrum lobelianum* or *Festuca varia* (Nakhutsrishvili 2012). On alluvial fans and close to the villages, young hay meadows occur on former organically fertilized arable fields characterized by *Hordeum brevisubulatum* (Tephnadze et al 2014). Older, nonfertilized and species richer hay meadows grow on steeper slopes and further away from the villages. We found no indication of the application of mineral fertilizers in our study region. For a detailed description of the study area, see Nakhutsrishvili (1999), Magiera et al (2013), and Tephnadze et al (2014).

Material and methods

Vegetation data

In summer 2014, the grassland vegetation within walking distance of 6 selected villages in the Kazbegi Valley (Stepantsminda, Gergeti, Pansheti, Sioni, Phkelsche, and Goristhikhe) was sampled in a stratified random design including low-, medium-, and high-productivity sites (strata). Exact locations of the plots, however, were chosen randomly. In order to avoid edge effects, we sampled only large homogeneous grassland patches at a minimum distance of 50 m from each other.

The vegetation composition of 90 plots, each covering 25 m^2, was assessed using the modified Braun-Blanquet scale and including all vascular plant species. The nomenclature follows The Plant List 1.1 (2013). Furthermore, we recorded the total vegetation cover as well as the cover of open soil and bare rocks. The cover percentage and height of the upper and lower herb layers were assessed separately. In order to estimate the cover fractions of the functional plant groups (grass [*Poaceae, Juncaceae, Cyperaceae*], legume [*Fabaceae*], and herb [all other species]), the Braun-Blanquet scale was transformed to cover percentages (r = 0.6%, + = 1.2%, 1 = 2.5%, 2m = 5%, 2a = 10%, 2b = 20%, 3 = 40%, 4 = 80%, 5 = 160%). We summarized the coverage of all species belonging to each functional group and used this as 100% coverage for comparison (van der Maarel 2007). We further identified

FIGURE 1 The study area in the Kazbegi region, Greater Caucasus, Georgia. (Map by Anja Magiera and
Tim Theissen)
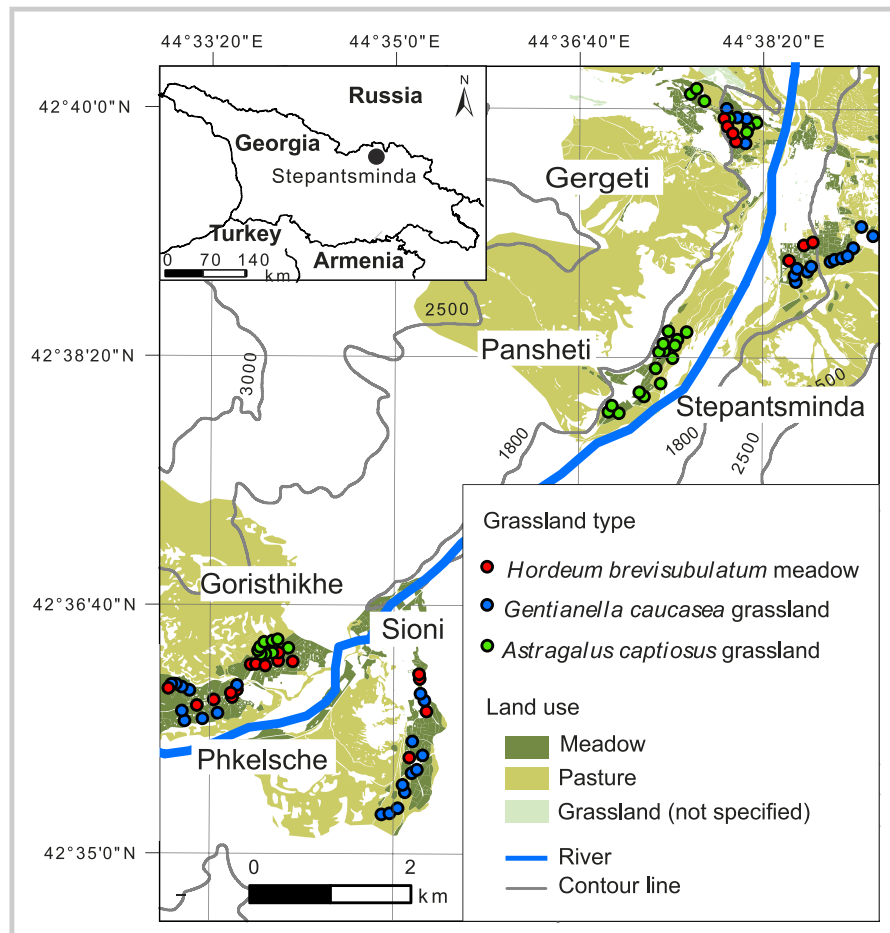
the most dominant (mean coverage of 5%) and frequent
(present in at least 30% of the vegetation relevés) species
within the 3 previously defined grassland vegetation types:
H. brevisubulatum meadow, *Gentianella caucasea* grassland,
and *Astragalus captiosus* grassland. In this paper we use the
term *grassland* where the land-use type is ambiguous
(haymaking and pasturing), whereas the term *meadow* is
used where haymaking occurs.

To depict the main floristic gradients, we performed a
nonmetric multidimensional scaling (NMDS; Kruskal 1964)
ordination. Ordination is a commonly used tool to reduce
the *n*-dimensional vegetation dataset to lower dimensional
floristic gradients. NMDS was chosen as an ordination
method because it is a robust, distance-based method that
accurately displays the ordinally scaled vegetation data. We
calculated an NMDS ordination with 3 dimensions using
the monoMDS function of the R package vegan 2.4-1
(Oksanen 2011). An NMDS was calculated for the plant
species composition of the plots based on Bray-Curtis
distances as a distance measure (Bray and Curtis 1957). The
NMDS axes were rotated by principal component rotation,
so that the new axis 1 pointed in the direction of the largest
variance (Clarke 1993).

Moreover, we tested structural vegetation parameters
for significant differences between the 3 grassland
vegetation types, using a Kruskal-Wallis analysis of
variance and a Nemenyi test for multiple comparisons of
rank sums implemented in the R package PMCMR 4.1.

Preprocessing of hyperspectral field spectrometric data, satellite imagery, and topographic data

We tested hyperspectral field spectrometric data and
multispectral satellite imagery, including vegetation
indices (VIs) and topographic data, for modeling grass,
herb, and legume coverage. Compared to the coarse
spectral resolution of multispectral data, commonly
including 3 to 10 discrete bands, the high spectral
resolution of hyperspectral data allows for a higher
flexibility in the selection of spectral features (Feilhauer et
al 2013). VIs are either ratios or linear combinations of
sensor bands that aim to enhance the vegetation signal
and allow conclusions on the status and condition of
vegetation (Jackson and Huete 1991).

In mid-July 2014, at the time of the highest biomass, we
acquired hyperspectral field spectrometric canopy

65

reflectance using a handheld field spectrometer (ASD HH2), covering a range of 325–1075 nm (750 wavelengths, with a 1-nm resolution) of the solar electromagnetic spectrum. The measurements were taken from the same 5 × 5-m plots as the vegetation relevés. To cover the entire plot, we took 4 measurements per plot with 5 repetitions (each measurement with an internal averaging of 50 spectra), totaling up to 20 spectra per plot, collected with a 25° conical field of view. The measurements were collected close to the solar noon, on days with clear sky and low wind speed. Atmospheric changes were accounted for by measuring relative to a white standard panel (Spectralon®, Labsphere Inc., North Sutton, NH), with a recalibration at least every 5 minutes. During preprocessing, the 20 spectra sampled per plot were averaged and filtered. A Savitzky-Golay filter with a quartic polynom and a filter length of 51 nm was used to smooth the spectra (Savitzky and Golay 1964).

Filtered field spectrometric reflectance measurements were used to test the applicability of hyperspectral sensors compared to multispectral sensors for modeling PFGs by simulating the bands of the sensors AISA Eagle (hyperspectral, 400–970 nm) and RapidEye (multispectral, 440–840 nm). PFGs have already successfully been predicted by AISA dual data as pollination types (Feilhauer et al 2016) and as vegetation types by moderate-resolution imaging spectroradiometer data (Sun et al 2008). Moreover, Lehnert et al (2013) have used hyperspectral data to discriminate grass from nongrass, but studies using multispectral data to model plant functional types are rather scarce. Both sensors were chosen because they cover a similar spectral range and offer high spatial resolution. To calculate the spectral signal of the AISA Eagle sensor, we cut the wavelengths of the AISA sensor (118 wavelengths) out of the hyperspectral field spectrometric data, whereas the function simulatoR (Feilhauer et al 2013) and the spectral response curve were used to simulate RapidEye reflectance.

Multispectral, space-borne imagery was acquired on 21 June 2014 by the RapidEye sensor. This sensor provides information on canopy reflectance in 5 bands (blue 440–510 nm, green 520–590 nm, red 630–685 nm, red edge 690–730 nm, and near infrared [NIR] 760–850 nm; Weichelt et al 2011). The imagery was orthorectified (product level 3-A) and converted to top-of-atmosphere reflectance. Differences in illumination due to the topography were corrected with a cosine topographic correction (Teillet et al 1982). Besides the 5 original bands, we included a set of previously published VIs in the analysis (Magiera et al 2017). The VIs were chosen because of their close relationship with plant characteristics. We used simple ratios, including red edge/red, NIR/red edge, red edge/NIR, NIR/red, and NIR/green. Moreover, we included the Atmospherically Resistant Vegetation Index 2 (ARVI; Kaufman and Tanre 1992), the Blue-Wide Dynamic Range Vegetation Index (BWDRVI; Gitelson 2004), the Modified Soil Adjusted Vegetation Index

(MSAVI; Qi et al 1994), the Enhanced Vegetation Index (EVI; Huete et al 1999), the Normalized Difference Vegetation Index (NDVI), and the Red Edge NDVI (Herrmann et al 2010). All indices were calculated by using the R raster package Version 2.5-8.

We included topographic data from a digital elevation model (DEM) with a 20 × 20-m resolution; we then calculated derivatives from that DEM, eastness, northness (Zar 1998), and slope (Horn 1981), as well as plan curvature, mean curvature, profile curvature, solar radiation, compound topographic index (Gessler et al 1995), heat load index (Mc Cune and Keon 2002), and surface relief ratio (Pike and Wilson 1971) with the Arc Map 10.2.1 tool box and the Geomorphometry and Gradient Metrics Toolbox version 1.0. The topographic data were selected to reflect those environmental conditions induced by the terrain that are known to impact vegetation characteristics (Moeslund et al 2013). We extracted the VIs and topographic variables for the positions of each vegetation relevé.

Modeling the vegetation structure

We tested the predictive power of hyperspectral canopy reflectance against multispectral reflectance (MR) for modeling PFGs. Moreover, we enhanced the multispectral model by using VIs and topographic variables.
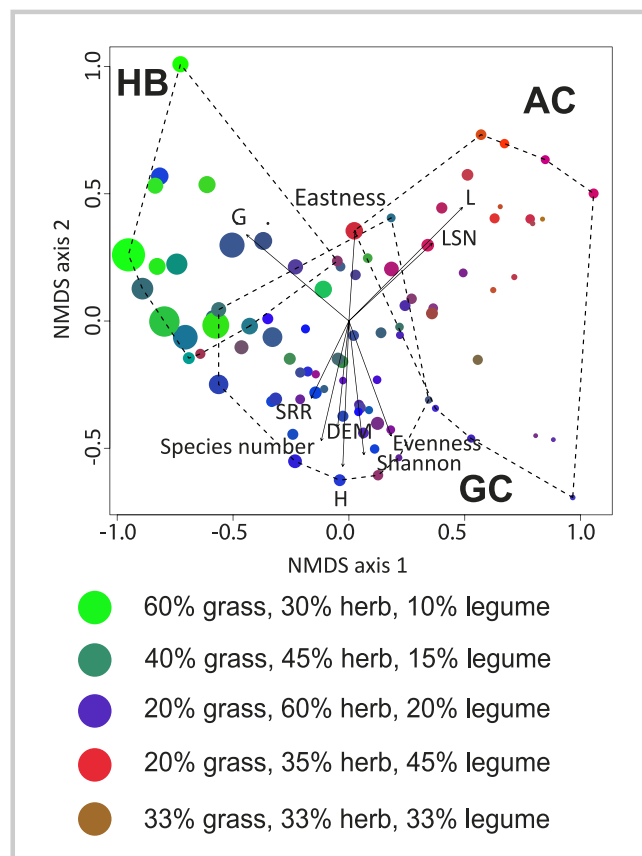
As a modeling technique, we chose random forest regression (Breiman 2001), an ensemble method belonging to bagged machine learning as implemented in the R package randomForest version 4.6-12 (Liaw and Wiener 2002). The random forest regression algorithm requires no assumption about data distributions; therefore, transformations are not necessarily needed (Breiman 2001; Liaw and Wiener 2002). The algorithm can capture nonlinear data structures that are often inherent in vegetation data. Moreover, it is robust towards outliers and can handle noise introduced by many predictor variables. The error rate of a random forest is assessed via out-of-bag estimation. The importance of a variable is assessed as a percentage increment of the mean square error (MSE) by permuting the out-of-bag data and the resulting error increase when one variable is left out (Liaw and Wiener 2002). Models were validated by a 100-fold bootstrapping procedure using the full dataset, as the sample size was relatively small. Adjusted R^2 as well as the root MSE were calculated for the relationship between predicted versus observed data. All 3 resulting maps were stacked and plotted in the red–green–blue (rgb) color code with r = legume coverage, g = grass coverage, and b = herb coverage.

Results

Grassland

The 90 vegetation relevés contained 177 plant species belonging to 35 families (26 graminoid species, 125

FIGURE 2 NMDS ordination diagram of the 2 main floristic gradients. The arrows point in the direction of the strongest change in topographic gradients (eastness, surface relief ratio [SRR], and elevation [DEM]) as well as vegetation-based gradients (grass [G], herb [H], legume [L], legume species number [LSN], species number, Shannon index, and evenness, as well as the vegetation types *H. brevisubulatum* meadow [HB], *G. caucasea* grassland [GC], and *A. captiosus* grassland [AC]). The length of the arrow represents the relationship between ordination and gradient, with a significance level of $P \leq 0.01$. Point size is fitted to grassland biomass (maximum biomass = 13.4 t*ha^{-1}, minimum biomass = 0.25 t*ha^{-1}).

variegatus, and *Poa alpina.* A high number of legume species, high legume coverage (eg *Medicago glutinosa* as a dominant species), and an overall low vegetation cover characterized the *A. captiosus* grassland.

Modeling PFGs

For modeling and mapping the selected PFGs for grass coverage, the most important predictor variables were the red-edge/NIR ratio, the ARVI, and the WDRVI. For herb coverage, the most important predictors were elevation, the red-edge band, and the profile curvature; for legume coverage, the main predictors were elevation, the NIR band, and the MSAVI.

The map shows that large areas of grassland were characterized by a high herb coverage, whereas grass-dominated patches were only small and established in close proximity to the settlements (Figure 3B, C, D). In contrast, patches dominated by legumes (mainly *A. captiosus*) covered larger areas mainly in the floodplains or on steep, south-exposed slopes characterized by open soil and bare rock (Figure 3C).

We further tested whether simulated hyperspectral field spectrometric reflectance, which matches the spectral characteristics of the AISA sensor, enhanced the model quality compared to simulated MR (RapidEye) or a mix of simulated MR, simulated VIs, and topographic variables as predictor variables.

The best-fitting models resulted from a mixed set of simulated MR, VIs, and topographic variables, whereas simulated HR performed equally well to the simulated MR (Table 2).

For the prediction of grass coverage, the blue and green bands played a key role when only MR was used as predictor (Figure 4). Eastness, elevation, and profile curvature were the most successful predictors in MR, VIs, and topographic parameters (TPs). Considering simulated AISA reflectance, wavelengths of 722–727 nm (red edge) resulted in the strongest increase in MSE. Wavelengths in the green part of the electromagnetic spectrum of light (511 nm) were strong predictors as well. Herb coverage was mostly predicted by the MR blue, green, and red bands, whereas elevation, eastness, profile curvature, and the red-edge/red ratio contributed the most to the MR, VI, and TP models. The variable importance for predicting legume coverage shows a high predictability of the blue band, the green band, and the NIR band in MR. Strong predictors in MR, VI, and TP were elevation, BWDRVI, and the NIR/green ratio. In HR, strong predictors were found in the blue (405 nm) region of the spectrum and the red edge (731 nm).

Discussion

Composition of grassland swards and management implications

The tested high-mountain grassland exhibited a vegetation structure common for unfertilized high-

herbaceous species, 22 fabaceous species, and 4 sedge species). The NMDS ordination accurately depicts the 2 main floristic gradients, with a stress level of 0.14 (Figure 2). Most of the original variation in the data (61%) is explained by the first NMDS axis; the second and third axes represent 26% and 0.5%, respectively. The color scheme represents the distribution of grass, herb, and legume in the rgb color space; that is, greenish points represent high grass coverage. Grassland vegetation is characterized by broad transitions, which explains the high species richness but makes it difficult to delineate grassland vegetation types.

The high grass coverage of the *H. brevisubulatum* meadow was accompanied by significantly higher total cover and yield (Table 1). Dominated by *H. brevisubulatum* and in the drier and stonier parts by *Agrostis vinealis, Trifolium repens, Ranunculus caucasicus,* and *Ranunculus ampelophyllus,* these meadows occurred on deep soils. The high herb coverage detected in the *G. caucasea* grassland was caused by species richness—mainly of herb species—and coverage more evenly distributed among single species; many species exhibited an average coverage below 15%. In contrast, dominance was established mainly by grassland matrix species shared with the *A. captiosus* grassland, such as *T. repens, Trifolium ambiguum, Bromus*

TABLE 1 Structural variables of the grassland types.[a]

	H. brevisubulatum meadow, $n = 23$			*G. caucasea* grassland, $n = 36$			*A. captiosus* grassland, $n = 31$		
	Median	25th Pctl	75th Pctl	Median	25th Pctl	75th Pctl	Median	25th Pctl	75th Pctl
Yield (Mg*ha^{-1})	5.97	4.80	7.98	2.61[b]	1.81	3.17	2.66[b]	2.13	3.16
Cover total (%)	100.00	98.00	100.00	95.50[b]	93.50	98.00	95.00[b]	90.00	96.00
Coverage litter (%)	0.00	0.00	0.00	0.50[b]	0.00	2.00	0.00[b]	0.00	2.50
Open soil (%)	0.00	0.00	2.00	2.50[b]	1.00	5.00	4.00[b]	2.00	5.00
Bare rock (%)	0.00[b]	0.00	0.00	0.00[b,c]	0.00	0.00	1.00[c]	0.00	4.50
Grass coverage	39.00[b]	31.00	54.00	21.00[c]	15.00	29.00	22.00[c]	19.00	29.00
Herb coverage (%)	43.00[b]	32.00	54.00	59.00	50.00	68.00	43.00[b]	32.00	50.00
Legume coverage (%)	12.00[b]	8.00	16.00	16.00[b]	9.00	23.00	35.00	18.00	43.00
Species number	28.00[b,c]	25.00	32.00	31.00[b]	28.00	35.00	27.00[c]	21.00	32.00
Shannon index	2.78[b]	2.49	2.92	2.99	2.82	3.18	2.69[b]	2.62	3.02
Evenness	0.83[b]	0.76	0.86	0.88[b,c]	0.86	0.91	0.84[c]	0.81	0.89

[a] Pctl, percentile.
[b] Homogeneous groups after a Kruskal-Wallis analysis of variance for multiple comparisons of rank sums $P \leq 0.01$.
[c] Homogeneous groups after a Nemenyi test for multiple comparisons of rank sums $P \leq 0.01$.

mountain grassland (Rudmann-Maurer et al 2008). Within all 3 tested vegetation types, herbs and legumes achieve high coverages compared to central European, nonintensively used grassland that is typically composed of 45% grass, 10% legume, and 45% herb coverage (Voigtlaender et al 1987). Grass coverage was significantly higher in *H. brevisubulatum* meadows in our dataset but was still within the range of unfertilized farmland, which has been almost lost in central Europe because of intensive farming practices but is in part conserved in high-mountain systems. Moreover, many species typical of central European grassland with a deep-growing root system, such as *Rumex obtusifolius, Festuca pratense*, and *Geranium sylvaticum*, were frequent in our data.

Higher herb coverage characterized the *G. caucasea* grassland, the species richest of all 3 grassland types. This was mostly caused by altering, low-intensity land use practices: although its biomass is moderate, *G. caucasea* grassland is mown whenever winter fodder is scarce; it is also pastured in spring with a low cattle density. This diverse, low-intensive land use without any mineral fertilizer has contributed to the species diversity of this grassland type. An abandonment of this management practice would lead to a considerable loss of high-mountain plant diversity (Maurer et al 2006).

Low species diversity, as analyzed for the legume-dominated *A. captiosus* grassland, and the typically scant vegetation coverage indicate areas potentially prone to erosion, mostly on southeast exposed slopes (Wiesmair et al 2016). Because of nutrient-poor soil conditions and drought, where erosion had started only a few species were able to establish themselves and maintain a vegetation cover. This highlights the importance of single species—especially the dominant *A. captiosus* with its immense (90 cm) root length and ability to provide nitrogen to co-occurring species—for mitigating erosion processes (Spehn et al 2002; Caprez et al 2011).

TABLE 2 Adjusted R^2 of the random forest models as determined via correlation between predicted and observed values in calibration and validation (bootstrapping).[a]

PFGs	HR in validation		MR in validation		MR, VI, TP in validation	
	Adjusted R^2	RMSE (%)	Adjusted R^2	RMSE (%)	Adjusted R^2	RMSE (%)
Grass coverage (%)	0.05	14.39	0.03	14.48	0.19	13.20
Herb coverage (%)	0.18	13.90	0.15	14.14	0.24	13.51
Legume coverage (%)	0.28	11.84	0.25	12.10	0.33	11.48

[a] HR, simulated hyperspectral reflectance; MR, simulated multispectral reflectance; VI, simulated MR vegetation indices, TP, topographic parameters; RMSE, root mean square error.

FIGURE 3 Modeled PFG coverage, with random forest models explaining 36% of the variance in the data, a root MSE in prediction (RMSEP) = 13% for grass coverage, a 25% explained variance and an RMSEP = 12% for herb coverage, and a 37% explained variance and an RMSEP = 11% for legume coverage in calibration, using MR, VIs, and TPs as predictors. Maps depict the villages: (A) Stepantsminda; (B) Gergeti; (C) Pansheti; (D) Goristhikhe and Phkelsche; (E) Sioni; (F) refers to the whole Kazbegi region. (Land use mapped by Tim Theissen)
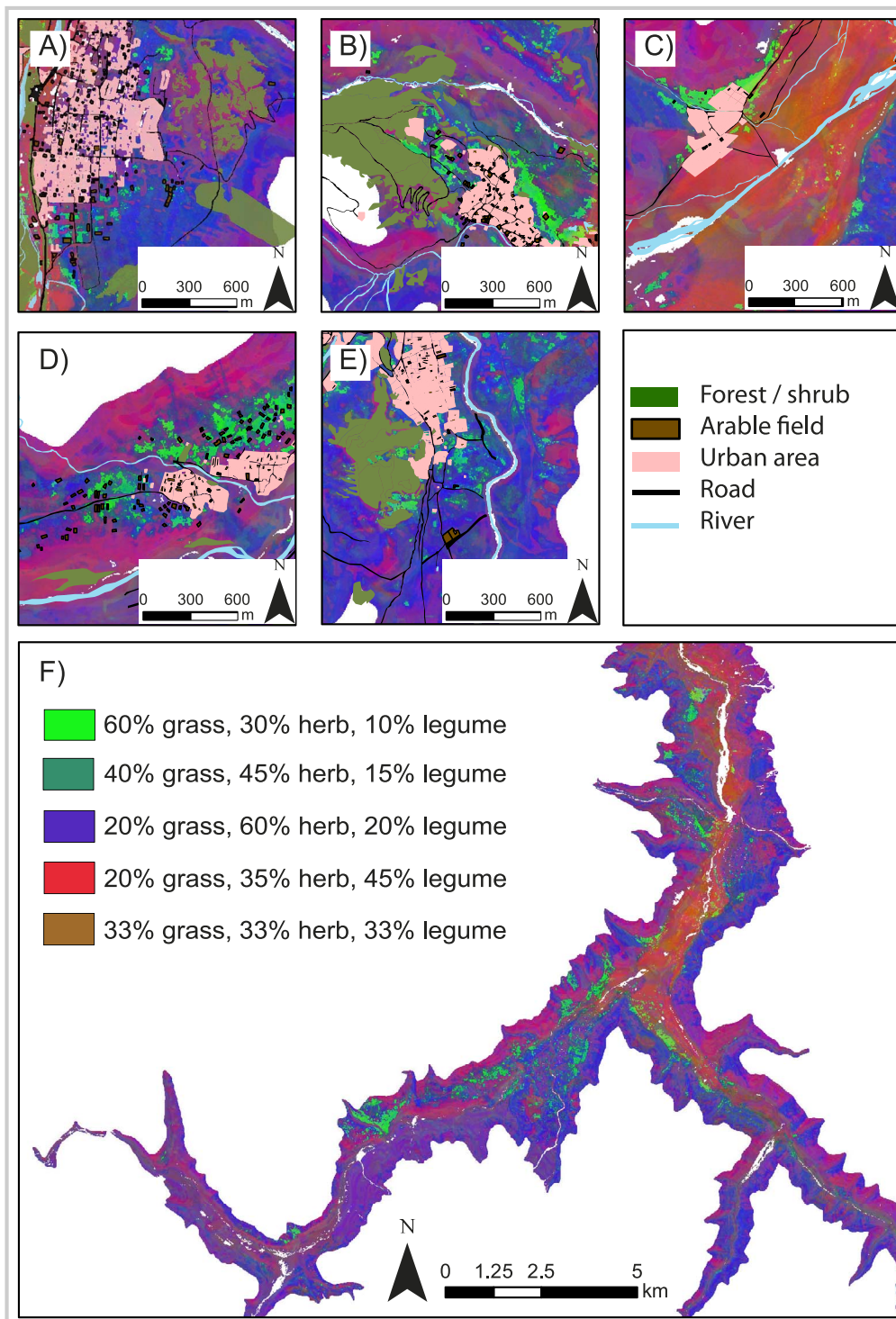
Modeling and mapping of PFGs

Even though the overall model quality was moderate, the calculated errors (11–15%) compare with the errors of visual field estimations; moreover, the resulting map depicts clear patterns of grass, herb, and legume coverage. The overall low variability in the dataset could explain the moderate model fits with a standard deviation for grass coverage of 14.74, for herb coverage of 15.05, and for

FIGURE 4   Variable importance calculated as percentage increment MSE using (A) simulated MR (RapidEye); (B) simulated MR (RapidEye), simulated VIs, and TPs; and (C) simulated HR (AISA) as predictors for grass, herb, and legume cover.
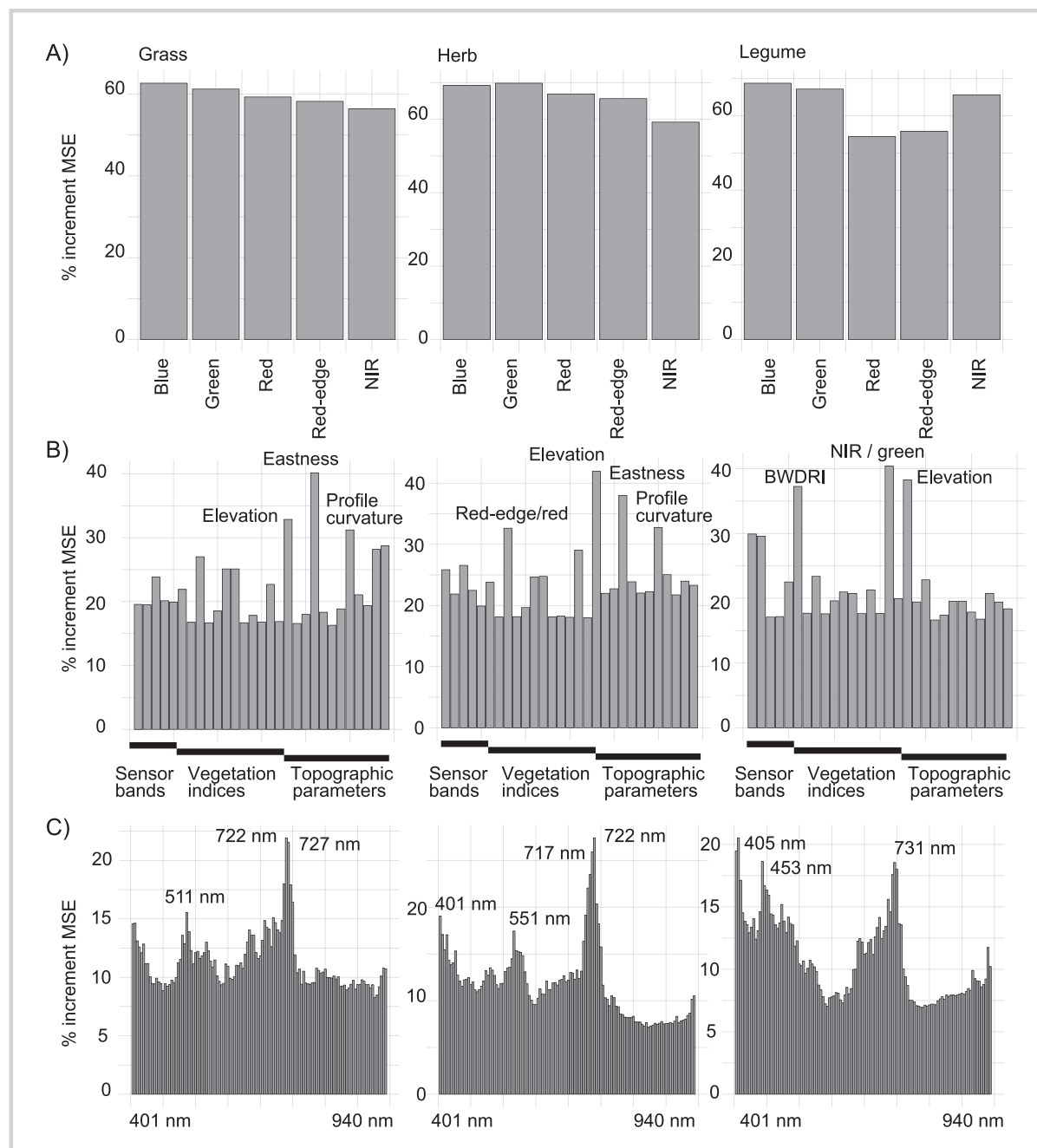
legume coverage of 14.15. Indeed, Biewer, Erasmi, et al (2009) found that in sown swards, varying sward age and the closely connected biomass distorted the relationship between VIs and grass and legume content.

VIs and topographic variables enhanced the model quality of the multispectral dataset, with elevation and profile curvature being the most important topographic variables because near-natural vegetation mainly follows topographic gradients (Moeslund et al 2013). Moreover,

important canopy characteristics, such as vegetation cover and the distribution of grass, herb, and legume species, relate to the topographic gradient, adding to the characteristic reflectance pattern (Pfitzner et al 2006).

We compared modeling results for predicting PFGs with HR and simulated multispectral data to test the potential of hyperspectral imagery for modeling PFGs. Using the resampled field, spectrometric data minimized the effects of illumination differences in multidate

comparisons (Nilson and Peterson 1994). Moreover, both datasets originated from the same spectra, unlike in a comparison of real satellite imagery where images are often recorded weeks apart. Therefore, we avoided inaccuracies introduced by rapid phenological development in high-mountain regions (Körner 2003). However, the spatial scale as a crucial sensor characteristic was not taken into account: the field of view of the spectrometer covers areas below 1 m^2, depending on the average height above ground, whereas the rescalable, airborne AISA Eagle imagery has varying pixel sizes ($<5 \times 5$ m) and the spaceborne RapidEye sensor delivers imagery with a pixel size of 5×5 m. The number of species in a pixel size increases with pixel size; we counteracted this problem by averaging spectra on 5×5-m plots. Using actual imagery might result in different model qualities (Magiera et al 2016; Meyer et al 2017).

The high spectral resolution of the hyperspectral data offered only a small advantage when modeling grass, herb, or legume coverage. Hyperspectral reflectance outperformed the MR by only 2–3%, whereas the combination of MR, VIs, and TPs explained another 10% of variance compared to the simple model with MR. However, hyperspectral imagery with a high spatial resolution is costly. The ability of MR to model floristic composition (Feilhauer et al 2013) as well as aboveground biomass and vegetation cover (Meyer et al 2017) is generally high. Both data types may be enhanced by including topographic variables, especially in a high-mountain study area. Moreover, spectral information from the shortwave infrared range, which is sensitive to the water and dry-matter content of the leaves, may add valuable information to the models (Feilhauer et al 2013). Such information is, however, available for only a few sensors with high spatial resolution (eg the commercial Worldview 3). Free multispectral imagery as delivered by Sentinel 2 could improve the model quality because it offers 3 red-edge, 2 NIR, and 2 shortwave infrared bands. However, the main pitfall of Sentinel 2 data is the rather coarse spatial resolution (20×20-m pixel size) compared to RapidEye (5×5-m pixel size). Further testing while using a broader spectral range, as provided by Sentinel 2, is therefore needed.

Conclusion

The high-mountain grassland of the Kazbegi region displays a unique species composition with a high coverage of herbs and legumes, resulting in a typical structure and vegetation cover. Mapping grass, herb, and legume coverage revealed the spatial limitation of grass-rich swards for haymaking and the domination of legumes on large areas with low vegetation coverage, which should be grazed with a low cattle density. Producing grass, herb, and legume cover maps could therefore aid in developing case-sensitive grassland management recommendations for a sustainable, economically and ecologically viable land use concept in these species-rich grasslands. To enhance model fits, further testing, including even stronger vegetation gradients and the addition of shortwave infrared wavelengths, is needed.

REFERENCES

Akhalkatsi M, Abdaladze O, Nakhutsrishvili G, Smith WK. 2006. Facilitation of seedling microsites by *Rhododendron caucasicum* extends the *Betula litwinowii* Alpine treeline, Caucasus Mountains, Republic of Georgia. *Arctic, Antarctic, and Alpine Research* 38:481–488.
Biewer S, Erasmi S, Fricke T, Wachendorf M. 2009. Prediction of yield and the contribution of legumes in legume-grass mixtures using field spectrometry. *Precision Agriculture* 10:128–144.
Biewer S, Fricke T, Wachendorf M. 2009. Determination of dry matter yield from legume-grass swards by field spectroscopy. *Crop Science* 49:1927–1936.
Blondel J. 2003. Guilds or functional groups: does it matter? *Oikos* 100:223–231.
Bray JR, Curtis JT. 1957. An ordination of the upland forest communities of southern Wisconsin. *Ecological Monographs* 27:325–349.
Breiman L. 2001. Random forests. *Machine Learning* 45:5–32.
Bühler C, Roth T. 2011. Spread of common species results in local-scale floristic homogenization in grassland of Switzerland. *Diversity and Distributions* 17:1089–1098.

Caprez R, Spehn E, Nakhutsrishvili G, Körner C. 2011. Drought at erosion edges selects for a "hidden" keystone species. *Plant Ecology & Diversity* 4:303–311.
Clarke KR. 1993. Non-parametric multivariate analyses of changes in community structure. *Austral Ecology* 18:117–143.
Feilhauer H, Doktor D, Schmidtlein S, Skidmore AK. 2016. Mapping pollination types with remote sensing. *Journal of Vegetation Science* 27:999–1011.
Feilhauer H, Thonfeld F, Faude U, He KS, Rocchini D, Schmidtlein S. 2013. Assessing floristic composition with multispectral sensors—A comparison based on monotemporal and multiseasonal field spectra. *International Journal of Applied Earth Observation and Geoinformation* 21:218–229.
Gessler PE, Moore, ID, Mc Kenzie NJ, Ryan PJ. 1995. Soil-landscape modelling and spatial prediction of soil attributes. *International Journal of Geographical Information Systems* 9:421–432.
Gitelson AA. 2004. Wide dynamic range vegetation index for remote quantification of biophysical characteristics of vegetation. *Journal of Plant Physiology* 161:165–173.
Herrmann I, Karnieli A, Bonfil DJ, Cohen Y, Alchanatis V. 2010. SWIR-based spectral indices for assessing nitrogen content in potato fields. *International Journal of Remote Sensing* 31:5127–5143.

Himstedt M, Fricke T, Wachendorf M. 2009. Determining the contribution of legumes in legume-grass mixtures using digital image analysis. *Crop Science* 49:1910–1916.

Homburger H, Hofer G. 2012. Diversity change of mountain hay meadows in the Swiss Alps. *Basic and Applied Ecology* 13:132–138.

Horn BKP. 1981. Hill shading and the reflectance map. *Proceedings of the IEEE* 69:14–47.

Huete A, Justice C, Van Leeuwen W. 1999. *MODIS Vegetation Index (MOD13). Algorithm Theoretical Basis Document.* Version 3. http://scholar.google.de/ scholar_url?url=https://pdfs.semanticscholar.org/2204/ b55a9ad69e8b69d19e88ad1f0e1f81a5d72b.pdf&hl=de&sa=X&scisig= AAGBfm3gtE1npDdV9-BcfBQGVWCIe3unuw&nossl=1&oi=scholarr&ved= 0ahUKEwie-dPU-vzZAhUHEJoKHY4UADEQgAMIJigAMAA; accessed on 21 March 2018.

Jackson RD, Huete AR. 1991. Interpreting vegetation indices. *Preventive Veterinary Medicine* 11:185–200.

Kaufman YJ, Tanre D. 1992. Atmospherically resistant vegetation index (ARVI) for EOS-MODIS. *IEEE Transactions on Geoscience and Remote Sensing* 30:261–270.

Ketskhoveli N, Kharadze AL, Ivanishvili MA, Gagnidze RI. 1975. *Botanical Description of the Georgian Military Road. (Tbilisi-Kazbegi-Ordjonikidze).* Leningrad, Russia: The Academy of Sciences of the Georgian SSR, The Institute of Botany.

Körner C. 2003. *Alpine Plant Life.* Berlin, Germany: Springer.

Körner C. 2004. Mountain biodiversity, its causes and function. *Ambio* 3:11–17.

Kruskal JB. 1964. Nonmetric multidimensional scaling: a numerical method. *Psychometrika* 29:115–129.

Lehnert LW, Meyer H, Meyer N, Reudenbach C, Bendix J. 2013. Assessing pasture quality and degradation status using hyperspectral imaging: a case study from western Tibet. *Proceedings of SPIE* 8887:88870I.

Lehnert LW, Meyer H, Meyer N, Reudenbach C, Bendix J. 2014. A hyperspectral indicator system for rangeland degradation on the Tibetan Plateau: A case study towards spaceborne monitoring. *Ecological Indicators* 39:54–64.

Liaw A, Wiener M. 2002. Classification and regression by randomForest. *R News* 2:18–22.

Lichtenegger E, Bedoschwili D, Hübl E, Scharf E. 2006. Höhenstufengliederung der Grünlandvegetation im Zentralkaukasus. *In: Verhandlungen der Zoologisch-Botanischen Gesellschaft in Österreich.* Wien, Austria: Zoologisch-Botanische Gesellschaft in Österreich, pp 43–81.

Magiera A, Feilhauer H, Otte A, Waldhardt R, Simmering D. 2013. Relating canopy reflectance to the vegetation composition of mountainous grasslands in the Greater Caucasus. *Agriculture, Ecosystems & Environment* 177:101–112.

Magiera A, Feilhauer H, Tephnadze N, Waldhardt R, Otte A. 2016. Separating reflectance signatures of shrub species - a case study in the Central Greater Caucasus. *Applied Vegetation Science* 19:304–315.

Magiera A, Feilhauer H, Waldhardt R, Wiesmair M, Otte A. 2017. Modelling biomass of mountainous grasslands by including a species composition map. *Ecological Indicators* 78:8–18.

Maurer K, Weyand A, Fischer M, Stöcklin J. 2006. Old cultural traditions, in addition to land use and topography, are shaping plant diversity of grasslands in the Alps. *Biological Conservation* 130:438–446.

Mc Cune B, Keon D. 2002. Equations for potential annual direct incident radiation and heat load. *Journal of Vegetation Science* 13:603–606.

Meyer H, Lehnert LW, Wang Y, Reudenbach C, Nauss T, Bendix J. 2017. From local spectral measurements to maps of vegetation cover and biomass on the Qinghai-Tibet-Plateau: Do we need hyperspectral information? *International Journal of Applied Earth Observation and Geoinformation* 55:21–31.

Moeslund JE, Arge L, Bøcher PK, Dalgaard T, Svenning JC. 2013. Topography as a driver of local terrestrial vascular plant diversity patterns. *Nordic Journal of Botany* 31:129–144.

Nakhutsrishvili G. 1999. The vegetation of Georgia (Caucasus). *Braun-Blanquetia* 15:5–74.

Nakhutsrishvili G. 2012. *The Vegetation of Georgia (South Caucasus).* Dordrecht, Netherlands: Springer.

Nilson T, Peterson U. 1994. Age dependence of forest reflectance: Analysis of main driving factors. *Remote Sensing of Environment* 48:319–331.

Oksanen J. 2011. Multivariate analysis of ecological communities in R: Vegan tutorial. http://cc.oulu.fi/~jarioksa/opetus/metodi/vegantutor.pdf; accessed on 25 July 2017.

Pfitzner K, Bollhöfer A, Carr G. 2006. A standard design for collecting vegetation reference spectra: Implementation and implications for data sharing. *Spatial Science* 52:79–92.

Pike RJ, Wilson SE. 1971. Elevation-relief ratio, hypsometric integral, and geomorphic area-altitude analysis. *Geological Society of America Bulletin* 82:1079–1084.

Pohl M, Alig D, Körner C, Rixen C. 2009. Higher plant diversity enhances soil stability in disturbed alpine ecosystems. *Plant and Soil* 324:91–102.

Psomas A, Kneubühler M, Huber S, Itten K, Zimmermann NE. 2011. Hyperspectral remote sensing for estimating aboveground biomass and for exploring species richness patterns of grassland habitats. *International Journal of Remote Sensing* 32:9007–9031.

Pyšek P, Šrutek M. 1989. Numerical phytosociology of the subalpine belt of the Kazbegi region, Caucasus, USSR. *Vegetatio* 81:199–208.

Qi J, Chehbouni A, Huete AR, Kerr YH, Sorooshian S. 1994. A modified soil adjusted vegetation index. *Remote Sensing of Environment* 48:119–126.

Rudmann-Maurer K, Weyand A, Fischer M, Stöcklin J. 2008. The role of landuse and natural determinants for grassland vegetation composition in the Swiss Alps. *Basic and Applied Ecology* 9:494–503.

Savitzky A, Golay MJE. 1964. Smoothing and differentiation of data by simplified least squares procedures. *Analytical Chemistry* 36:1627–1639.

Spehn EM, Scherer-Lorenzen M, Schmid B, Hector A, Caldeira MC, Dimitrakopoulos PG, Finn JA, Jumpponen A, O'Donnovan G, Pereira JS, Schulze ED, Troumbis AY, Körner C. 2002. The role of legumes as a component of biodiversity in a cross-European study of grassland biomass nitrogen. *Oikos* 98:205–218.

Sun W, Liang S, Xu G, Fang H, Dickinson R. 2008. Mapping plant functional types from MODIS data using multi-source evidential reasoning. *Remote Sensing of Environment* 112:1010–1024.

Tasser E, Tappeiner U. 2002. Impact of land use changes on mountain vegetation. *Applied Vegetation Science* 5:173–184.

Teillet PM, Guindon B, Goodenough DG. 1982. On the slope-aspect correction of multispectral scanner data. *Canadian Journal of Remote Sensing* 8:84–106.

Tephnadze N, Abdaladze O, Nakhutsrishvili G, Simmering D, Waldhardt R, Otte A. 2014. The impacts of management and site conditions on the phytodiversity of the upper montane and subalpine belts in the Central Greater Caucasus. *Phytocoenologia* 44:255–291.

The Plantlist. 2013. The Plantlist. Version 1.1. http://www.theplantlist.org; accessed on 16 February 2016.

van der Maarel E. 2007. Transformation of cover-abundance values for appropriate numerical treatment—Alternatives to the proposals by Podani. *Journal of Vegetation Science* 18:767–770.

Voigtlaender G, Jacob H, Boeker P. 1987. *Grünlandwirtschaft und Futterbau.* Stuttgart, Germany: Ulmer.

Weichelt H, Rosso P, Marx A, Reigber S, Douglass K, Heynen M. 2011. *White paper: The RapidEye red edge band.* https://www.google.de/url?sa=t&rct= j&q=&esrc=s&source=web&cd=1&ved= 0ahUKEwienMvFgP3ZAhXjYpoKHaMoAZMQFggnMAA&url=https%3A%2F% 2Fresa.blackbridge.com%2Ffiles%2F2014-06%2FRed_Edge_White_Paper. pdf&usg=AOvVaw3_nRmurPYDDQsS4wF6qGgs; accessed on 21 March 2108.

Wiesmair M, Feilhauer H, Magiera A, Otte A, Waldhardt R. 2016. Estimating vegetation cover from high-resolution satellite data to assess grassland degradation in the Georgian Caucasus. *Mountain Research and Development* 36:56–65.

Wiesmair M, Otte A, Waldhardt R. 2017. Relationships between plant diversity, vegetation cover, and site conditions: Implications for grassland conservation in the Greater Caucasus. *Biodiversity and Conservation* 26:273–291.

Zar JH. 1998. *Biostatistical Analysis.* 4th edition. New York, NY: Prentice Hall.

Zha Y, Gao J, Ni SX, Liu YS, Jiang JJ, Wei YC. 2003. A spectral reflectance-based approach to quantification of grassland cover from Landsat TM imagery. *Remote Sensing of the Environment* 87:371–375.